Cement and Concrete Research 41 (2011) 184–190

Contents lists available at ScienceDirect

Cement and Concrete Research

journal homepage: http://ees.elsevier.com/CEMCON/default.asp

An ESEM investigation of latex film formation in cement pore solution

M. Gretz, J. Plank *

Institute for Inorganic Chemistry, Technische Universität München, Lichtenbergstr. 4, 85747 Garching, Germany

ARTICLE INFO

Article history:
Received 4 March 2010
Accepted 10 November 2010

Keywords:
Cement (D)
Latex film formation
Polymers (D)
Pore solution (B)
SEM (B)

ABSTRACT

Environmental scanning electron microscopy (ESEM) and complementary methods were employed to study the time dependent film formation of a latex dispersion in water and cement pore solution. First, a model carboxylated styrene/*n*-butyl acrylate latex dispersion possessing a minimum film forming temperature (MFFT) of 18 °C was synthesized in aqueous media via emulsion polymerization. Its film forming property was at a temperature of 40 °C, studied under an ESEM. The analysis revealed that upon removal of water, film formation occurs as a result of particle packing, particle deformation and finally particle coalescence. Film formation is significantly retarded when the latex dispersion is present in cement pore solution. This effect can be ascribed to adsorption of Ca^{2+} ions onto the surface of the anionic latex particles and to interfacial secondary phases. This layer of adsorbed Ca^{2+} ions hinders interdiffusion of the macromolecules and subsequent film formation of the latex polymer.

1. Introduction

Latex dispersions are widely used for modification of cement-based mortars and concretes [1,2]. They allow to improve some undesired properties of hardened cement such as brittleness and low flexural strength. Additionally, cohesion and adhesion of the fresh and hardened mortars and concretes are significantly enhanced. These effects are owed to the formation of polymer films which result from the coalescence of latex particles when water is consumed by cement hydration and evaporation. The latex polymers which are most common in the construction industry are based on ethylene/vinyl acetate or styrene/acrylate chemistry [2].

Studies on the film forming process of latex polymers represent a field of intense research since many years [3,4]. Latex film formation is a process which entails several steps. It starts from an aqueous latex dispersion and ultimately results in a homogeneous polymer film. A schematic representation of the film formation process in water as solvent is shown in Scheme 1. Generally, the film forming process can be viewed as a succession of those four steps:

In Stage I, the latex particles are randomly dispersed in the solvent. When water is removed from this dispersion, ordering and packing of the particles takes place (stage II). The particles are in contact with each other whereby the interstitial spaces are filled with solvent. As water evaporation and consumption progresses, an ordered array of hexagonal deformed latex particles is formed (stage III). For latex dispersions exhibiting a hydrophilic surface, particle deformation results into polyhedral cells separated by hydrophilic layers (transition stage III*) [5]. Some authors present that between stage II and III, an intermediate stage (II*) exists which is characterized by a randomly packed array of deformed particles which are surrounded by water-filled interspaces [6]. Finally, in stage IV a molecularly homogeneous polymer film is formed as a result of particle coalescence stemming from polymer interdiffusion and break up of hydrophilic interlayers. This process requires that the ambient temperature is above the minimum film forming temperature (MFFT). MFFT depends on the monomer composition of the latex particles and is influenced by other additives (e.g. emulsifier) used in the emulsion polymerization process. Experimentally, it is determined on a so-called *Kofler* bench. Closely linked to MFFT is the glass transition temperature (T_g) of a latex dispersion. It represents the temperature at which an initially soft and flexible latex polymer film becomes brittle and hard. For a given polymer, T_g can be calculated using the *Fox* equation [7], or it is measured by differential scanning calorimetry (DSC).

Today, the film forming process occurring in water is understood sufficiently. There are, however, only few reports on the effect of electrolytes (e.g. salt) on the film formation. Such condition is however prevalent when latex polymers are used in cement-based building materials such as tile adhesives, self-levelling compounds, polymer concrete etc.

According to *Chandra* and *Flodin* styrene methacrylate dispersions lose their film forming ability when blended with $Ca(OH)_2$ [8]. Using a sorption balance Erkselius et al. found a significantly reduced drying rate for a methyl methacrylate-methyl acrylate latex copolymer when surfactants and salts were present [9]. Hence, it becomes obvious that latex film formation is highly sensitive to ambient conditions, such as temperature, pH or type and concentration of ions present in solution. In another work, Jenni and Zurbriggen present that film formation of a polyvinylalcohol coated redispersible latex powder is accelerated in

---

* Tel.: +49 89 289 13151; fax: +49 89 289 13152.
E-mail address: sekretariat@bauchemie.ch.tum.de (J. Plank).

0008-8846/$ – see front matter © 2010 Elsevier Ltd. All rights reserved.
doi:10.1016/j.cemconres.2010.11.005

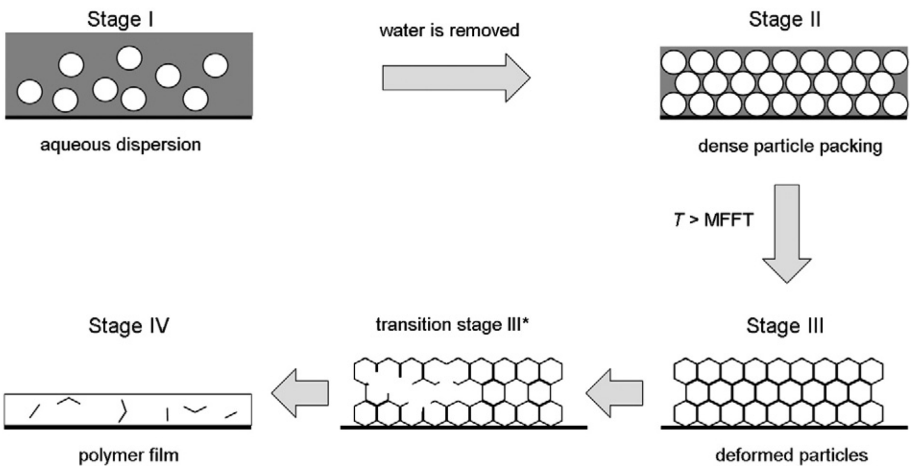

Scheme 1. Schematic representation of stages I to IV occurring during the process of film formation from an aqueous polymer latex dispersion.

cement pore solution [10]. This effect is ascribed to crosslinking between slightly anionic latex particles instigated by Ca^{2+} ions. Obviously, this finding contradicts those of Chandra and Flodin [8] and of Erkselius et al. [9]. Thus, it was our goal to clarify how our anionic styrene/n-butylacrylate dispersion will behave in cement pore solution. Chandra and Flodin found that a styrene methacrylate dispersion loses its film forming ability when blended with $Ca(OH)_2$ while Erkselius et al. report a significant reduced drying rate for a methyl methacrylate–methacrylate dispersion when salts were present. These results are in perfect agreement with our own findings.

In cement pore solution, a highly alkaline pH (~12.5–14) and a noticeable concentration of mono- and divalent anions and cations exists. Depending on the water-to-cement ratio (w/c) of the mortar or concrete, the total concentration of all electrolytes may reach as high as 30 g/L, with SO_4^{2-} and K^+ concentrations running particularly high (~7–10 g/L and ~6–12 g/L, resp.) [7]. Whereas, Na^+ and Ca^{2+} exhibit relatively low concentrations (~2–5 g/L and ~1 g/L, resp.). Consequently, a cement pore solution represents a special environment for the coalescence and film formation of the latex polymer. A noticeable influence on the mechanism and kinetics of the film forming process can be expected.

Generally, the film formation process of the latex polymers can be investigated by means of environmental scanning electron microscopy (ESEM). This technique offers the possibility to study wet and non-conductive samples in their original state [11]. The vacuum system employed in the ESEM instrument provides a relatively low vacuum above the sample placed in the specimen chamber at a water vapour pressure of 1–10 mbar, while the gun and the column remain at high vacuum ($\sim 9 \times 10^{-8}$ mbar) [12]. Through this setup, dehydration of the specimen can be avoided if the atmosphere surrounding the sample remains saturated with water vapour. This can be achieved by cooling of the sample and by using an individual pump-down sequence [13].

Here, we present an environmental scanning electron microscopic study of the time dependent film formation of an anionic latex polymer. The behaviour in water and synthetic cement pore solution as solvent was compared. For this purpose, an anionic latex was synthesized by conventional emulsion polymerization technique. The latex polymer was based on styrene/*n*-butyl acrylate chemistry. Additionally, methacrylic acid was incorporated as comonomer to provide enhanced colloidal stability. Film formation was tracked by environmental scanning electron microscopy. Droplets of latex polymer at 5 wt.% concentration dispersed in water or synthetic cement pore solution were placed on an aluminium disk and transferred into a dry-box with controlled climate conditions. There, they were allowed to dry at 40 °C and 25% relative humidity over a period of up to 3 days. From these samples, individual probes were transferred into the microscope for investigation at different times. A special pump-down sequence was developed to avoid additional drying and dehydration while vacuum setting in the sample chamber of the ESEM instrument. Time dependent film formation was observed and the behaviour of latex in water and cement pore solution was compared.

2. Materials and methods

2.1. Materials

Styrene, *n*-butyl acrylate, methacrylic acid, sodium peroxo disulphate, calcium sulphate dihydrate, potassium hydroxide and sodium and potassium sulphate were purchased from Merck, Darmstadt/Germany. Marlon® A 375 emulsifier (an alkyl benzenesulphonate anionic emulsifier) was provided by Sasol, Hamburg/Germany. Prior to their use, the monomers were purified by treatment with 1 wt.% aqueous NaOH (for styrene) or NaOH/Na_2CO_3 (1:1 wt./wt., for *n*-butyl acrylate) to remove inhibitors. All other chemicals were utilised without further purification. Ultrapure water (resistivity > 18 MΩ cm) was used for all experiments.

2.2. Preparation and characterization of the latex polymer

The latex dispersion was prepared by semi batch emulsion polymerization in a five neck glass flask equipped with a mechanical stirrer, reflux condenser, N_2 inlet, dosing unit and a temperature controller. First, the flask was charged with an aqueous solution of the initiator (1.3 g $Na_2S_2O_8$) in 72 mL ultrapure water and heated to 80 °C. Next, an emulsion prepared from water, styrene (S), *n*-butyl acrylate (BA), methacrylic acid (MAA) and the surfactant (emulsifier) was added within 3 h at a constant feed rate to the initiator solution using a flexible tube pump (Ismatec MCP, Wertheim/Germany). Composition and characteristic properties of the latex sample are presented in Table 1.

The synthesized white latex dispersion was purified from residual monomers by steam distillation. Final polymer content was 43 wt.%.

Particle size was determined by dynamic light scattering (DLS) with a Zetasizer Nano ZS (Malvern Instruments, Workestershire/UK). Measurement of the electrophoretic mobility was conducted on the

Table 1
Starting materials and properties of the synthesized anionic latex polymer.

Monomers S/BA/MAA (g)	Emulsifier (g)	Water (g)	Particle size (nm)	MFFT (°C)	T_g (°C)	Zeta potential (mV)
63/63/1.5	1.3	46	239	18	24	−55

same instrument. Mobility was converted into a value for zeta potential by using the *Smoluchowski* relation.

Streaming potential was determined using a Mütek PCD 03 pH (BTG, Herrsching/Germany) particle charge detector. For each measurement, 10 mL of 0.01 wt.% latex suspension were used. pH was adjusted to 12.6 with 0.01 mol/L aqueous sodium hydroxide solution. Behaviour in the presence of calcium, sodium and potassium ions was studied by adding 0.25 mol/L aqueous $CaCl_2$, NaCl or KCl solutions, respectively.

Glass transition temperature (T_g) was measured on a differential scanning calorimeter (DSC) Maia F3 from Netzsch, Selb/Germany. Minimum film formation temperature (MFFT) was determined on an MFFT Bar Thermostair II instrument from Coesfeld Materialtest, Dortmund/Germany.

2.3. Preparation of synthetic cement pore solution

Time dependent film formation of the latex was studied in water and synthetic cement pore solution (SCPS) as solvents. SCPS was composed based on characteristic ion concentrations present in pore solutions of ordinary Portland cement at w/c ratios of ~0.5 [14]. The pore solution was prepared by dissolving 1.72 g $CaSO_4\ 2H_2O$, 6.96 g Na_2SO_4, 4.75 g K_2SO_4 and 7.12 g KOH in deionised water. First, 1.72 g of $CaSO_4\ 2H_2O$ were dissolved in 700 mL of water under vigorous stirring. 150 mL of the prepared $CaSO_4$ solution were used to dissolve 6.96 g of Na_2SO_4. Upon complete dissolution of the sodium sulphate, the solution was combined with the remaining $CaSO_4$ solution. Next, 4.75 g of K_2SO_4 were added and solved. Afterwards, 7.12 g KOH dissolved in 150 mL of water were introduced into this mixture. Finally, water was added to a volume of 1 L. This method produces a clear, stable liquid free of precipitate which incorporates the ion concentrations displayed in Table 2. pH of the SCPS was 12.6.

2.4. ESEM test protocol

Environmental scanning electron microscopy (ESEM) allows the observation of wet samples in their native state. In order to obtain valid results, however, careful control of the instrument parameters which create the exposure conditions of the sample is essential.

While the atmosphere in the sample chamber is decreased from ambient conditions to a water vapour pressure of ~7.5 mbar (this corresponds to 100% relative humidity at 3 °C sample temperature), the sample has to be maintained in its wet and original state. To achieve this, a specific pump-down sequence is required. It consists of several evacuation and water vapour addition steps to ensure that the water is retained in the sample.

Further, when working with an environmental scanning electron microscope, another important aspect is to prevent sample dehydration during imaging. Therefore, a saturated water vapour atmosphere has to be perpetuated in the specimen chamber. From the temperature dependent water vapour pressure curve it becomes obvious that at room temperature, a water vapour pressure of ~18 mbar is required to achieve saturation of the atmosphere with water vapour and thus prevent any dehydration. This is, however, not possible from the instrumental setup. To overcome this problem, the sample was cooled to a temperature of 3 °C. There, a saturated water atmosphere exists at a pressure of ~7.5 mbar. To allow high resolution imaging, the pressure has to be lowered further to ~6.5–5 mbar (this corresponds to 90–60% relative humidity). Under those conditions, a very minor amount of the surface water will be removed, but the bulk of the sample will remain in its original wet state, as has been reported by other authors before [15].

Cooling of the sample to a temperature of 3 °C would prevent film formation for the latex polymer investigated here since this temperature is far below the minimum film forming temperature of this latex which is 18 °C (Table 1). To solve this problem, all latex samples were stored in a dry box outside the ESEM instrument at a temperature of $T = 40 \pm 2$ °C and at a relative humidity of 25 ± 5%. This temperature is well above MFFT of the latex sample studied here. For ESEM analysis, the samples were transferred into the microscope and the pump-down sequence presented in Table 3 was applied to establish a water vapour atmosphere close to saturation as has been described before.

The points presented above illustrate that careful and conscious selection of instrument parameters and test conditions is critical to obtain valid results which are close to application conditions. Ignoring this fact allows the production of practically any result, because the ESEM instrument offers multiple ways which can manipulate imaging conditions.

Latex film formation was investigated using a dispersion possessing a polymer content of 5 wt.%. Solvent was water or synthetic cement pore solution. 20 μL of the latex polymer were deposited on a concave Al disk supplied as sample container for the ESEM instrument by FEI, Eindhoven/Netherlands, resulting in droplets possessing a layer thickness of ~300 μm. The samples were stored in a dry box at 40 ± 2 °C and 25 ± 5% relative humidity. For microstructural analysis and investigation of the latex film forming process, samples were transferred into an XL-30 FEG (FEI, Eindhoven/Netherlands) environmental scanning electron microscope (ESEM) equipped with a Peltier cooling stage and a gaseous secondary electron detector. Al disks were placed on the cooling stage in the microscope chamber at a temperature of 3 °C. A gentle pump-down sequence was performed to prevent water evaporation from the sample while reducing the pressure in the specimen chamber. During this process which takes about 3 min, air is progressively replaced by water vapor. The individual steps of the pump-down procedure are summed up in Table 3.

Once the water vapour purging cycle was completed, a water vapour pressure of 5.3–6.0 mbar was set for wet samples. This condition provided suitable imaging conditions. Dry samples were investigated under reduced water vapour pressure condition (1.0 mbar). Imaging was carried out at accelerating voltages of 10.0 or 25.0 kV, respectively, and at working distances of 8–11 mm.

3. Results and Discussion

The results of the microscopic investigations are presented here. First, film formation of the latex polymer dispersed in water will be discussed. This will be compared with the results for latex film formation obtained in synthetic cement pore solution.

Table 2
Concentration of ions present in the model cement pore solution used in the study.

Ion	Concentration (g/L)
K^+	7.1
Na^+	2.2
Ca^{2+}	0.4
SO_4^{2-}	8.2

Table 3
Pump-down sequence for ESEM imaging of latex polymer samples.

Step	Water vapour pressure *p* (mbar)
1	atm. → 8.5
2	8.5 → 12.5
3	12.5 → 8.5
4	8.5 → 7.5

Note: Dew point of water at 3 °C is ~7.5 mbar.

3.1. Film formation of latex in water

The ESEM image of the latex dispersed in water (c = 5 wt.%) exhibits individual monodisperse particles. Their apparent size corresponds with the value of 239 nm measured prior to the ESEM imaging by dynamic light scattering. The latex particles are randomly distributed and no agglomerates can be observed. Although some of the polymer particles are in contact with each other, no significant deformation has yet occurred. This provides evidence that the latex is still present in its original state (stage I).

Individual particles are surrounded by bright haloes which can be ascribed to hydrated surfaces. Owed to the hydrophilic surface of the latex which stems from incorporation of methacrylic acid and emulsifier into the polymer, water evaporation from the surface is hindered. These bright haloes will disappear when water vapour pressure is reduced to $p < 5$ mbar, indicating premature dehydration of the sample.

The latex sample depicted in Fig. 1 was removed from the ESEM instrument, ~5 μL were dispersed in 1 mL water and its particle size was measured using dynamic light scattering. The size distribution for the latex particles exposed to ESEM imaging had not changed much. A d_{50} value of ~239 nm found for the dispersion prior to ESEM imaging compared favourably with ~240 nm after ESEM treatment. This confirms that particle coalescence and film formation have not yet occurred.

For the latex sample studied here, stage II of the film forming process occurs about 30 min after the droplet has been placed on the disk and was stored at 40 °C (Fig. 2). Water evaporation causes the particles now to come into close contact with each other. The ESEM image also shows that the particle packing is not always regular, and that defects and grain boundaries exist. Yet, the latex particles still exhibit spherical shapes, and practically no deformation has occurred. According to Fig. 2, the particles are still surrounded by bright haloes, indicating that residual water is still captured on the hydrophilic surfaces of the latex spheres.

In Fig. 2, an interesting observation is that some latex particles exhibit a particularly bright halo. On the surface of those particles significant segregation of emulsifier and electrolytes is observed.

Continued water evaporation at temperatures above the MFFT causes particle deformation and subsequent polymer interdiffusion. The latex spheres attain a hexagonal shape and form an ordered array similar to honey-combs. The styrene/*n*-butyl acrylate latex studied here is hydrophobic by nature, but the particles are separated by hydrophilic membranes existing on their surface. This layer results from incorporation of methacrylic acid into the polymer and the presence of emulsifier submerged into the surface with its hydrophobic tail. Particle coalescence can only occur after removal of these hydrophilic layers, allowing direct contact between two adjacent particles. As reported by Joanicot et al., membrane separation causes a large area of interface (~30 m^2/g in their study) between the hydrophobic and hydrophilic components which is not representing the state of lowest free energy for the dispersion [16]. Therefore, in the drying process the system will attempt to reduce this interface area by segregating the hydrophobic and hydrophilic components. Once segregation and fragmentation have occurred, a continuous latex film can be formed by interdiffusion of polymer chains. At this point, all memory of the original particles is lost.

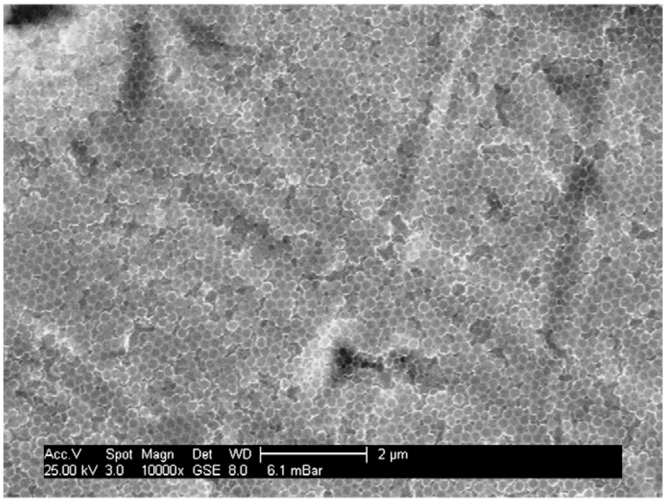

Fig. 1. ESEM micrograph of the latex (c = 5 wt.%) dispersed in water (*t* = 0 min, stage I). Imaging conditions: *T* = 3 °C; *p* = 6.1 mbar; *U* = 25 kV; magnification: 10000×.

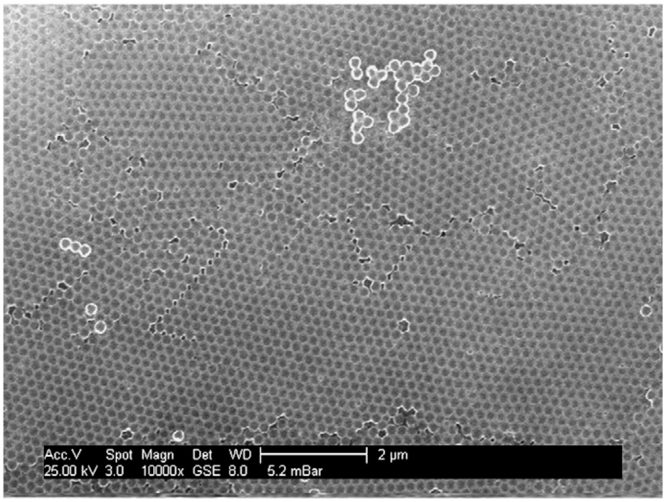

Fig. 2. ESEM micrograph of the latex sample after 30 min storage at 40 °C/25% r. h., evidencing increased particle ordering stemming from water evaporation (stage II). Imaging conditions: *T* = 3 °C; *p* = 5.2 mbar; *U* = 25 kV; magnification: 10000×.

For the latex polymer studied here, fragmentation of the hydrophilic layers and beginning coalescence can be observed about 60 min after beginning of sample storage. At this time, the latex is in stages III* and IV of the film forming process, as is evidenced by the ESEM micrograph displayed in Fig. 3. Again, it can be observed that in the array of densely packed latex spheres, several regions exist where latex particles exhibit a particularly bright haloe. There, hydrophilic components such as salts (e.g. from the initiator), emulsifier and

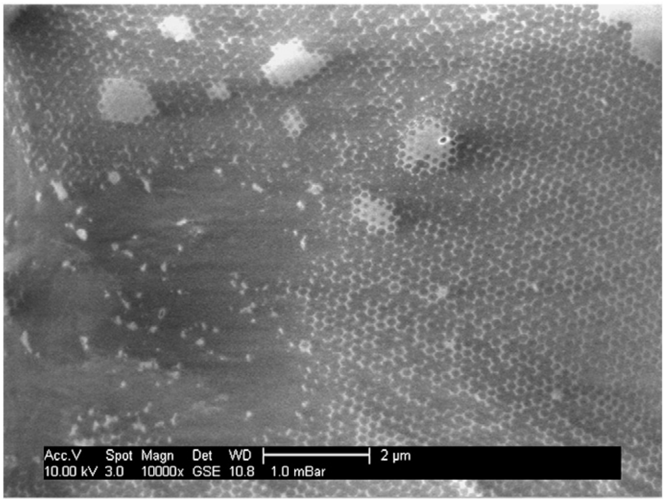

Fig. 3. ESEM micrograph of the latex sample after 60 min storage at 40 °C/25% r. h., evidencing fragmentation of hydrophilic membranes and partial film formation (stages III* and IV). Imaging conditions: *T* = 3 °C; *p* = 1.0 mbar; *U* = 10 kV; magnification: 10 000×.

water concentrate. They cannot be integrated into the latex polymer film, and therefore are still visible as separate particles scattered over the surface of the coalesced polymer film (see left section in Fig. 3). A detailed view of latex particles possessing a particularly thick hydrophilic layer amidst a mostly coalesced polymer film is exhibited in Fig. 4.

Film formation of the aqueous polymer dispersion is completed approximately after 4 h. Then, a continuous polymer film with hydrophilic residues on its surface is observed (Fig. 5).

The ESEM investigation presented here with water as solvent allows to conclude that for the synthesized latex polymer, the mechanism of film formation is in good agreement with the well known model which encompasses a four step process.

3.2. Film formation in cement pore solution

During hydration of cement, several ions namely K^+, SO_4^{2-}, Ca^{2+}, Na^+ and OH^- are released into the pore solution which possesses a pH >12. Thus, the surface properties of the polymer latex may be strongly affected by pH and the type and concentration of the electrolytes present there. Consequently, influence of these conditions on latex film formation needs to be studied.

Here, latex film formation was investigated using a synthetic cement pore solution (SCPS) possessing a pH of 12.6. SCPS was preferred over an actual cement paste filtrate because of the absence of fine cement particles not retrieved by centrifugation which may influence the microscopic results. The polymer latex was dispersed in the synthetic cement pore solution at a concentration of 5 wt.%. This addition corresponds to a latex dosage of approximately 2.5% by weight of cement in a mortar prepared at a w/c ratio of 0.5. Thus, it is within the range of typical application dosages. Several samples were deposited on Al disks and stored in a dry box at $T = 40 \pm 2$ °C and at a relative humidity of 25 ± 5%. For each ESEM imaging, an individual sample was transferred into the instrument and discarded after imaging. This way it was ensured that particle coalescence could proceed undisturbed under the constant conditions existing in the dry box. The same pump-down sequence was applied for chamber evacuation and water vapour atmosphere setting as described before.

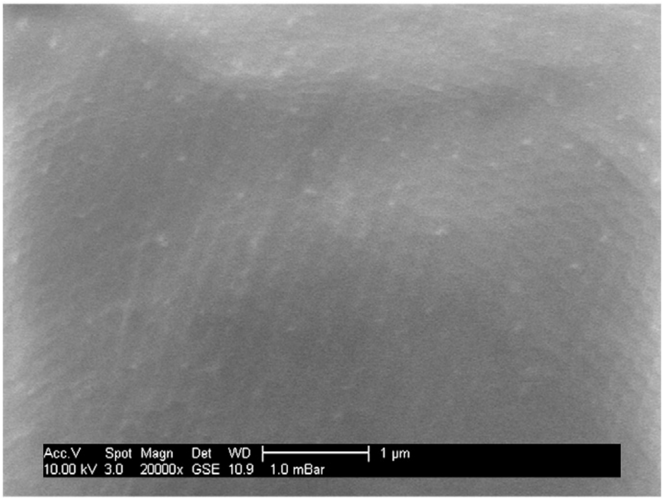

Fig. 5. ESEM micrograph exhibiting the polymer film obtained after 6 h of storage at 40 °C. Imaging conditions: $T = 3$ °C; $p = 1.0$ mbar; $U = 10$ kV; magnification: 20 000×.

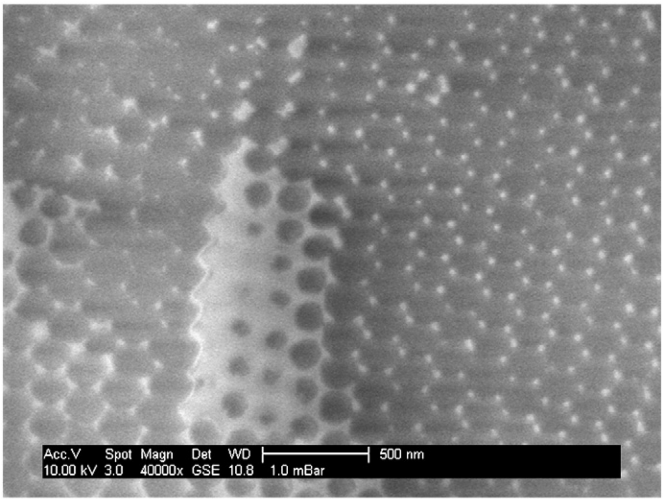

Fig. 4. ESEM micrograph exhibiting a detailed view of latex particles possessing a thick bright hydrophilic layer separated from a mostly coalesced polymer film. Note that on the polymer film as well, small amounts of segregated hydrophilic materials (emulsifier, salts) are visible. Imaging conditions: $T = 3$ °C; $p = 1.0$ mbar; $U = 10$ kV; magnification: 40 000×.

For stage I of the latex film formation, results obtained in synthetic cement pore solution were comparable with those described for water as solvent. The latex exhibits randomly distributed individual particles. Here as well, no deformation of particles was found. In this stage I, water evaporation has not yet occurred. The salts are still solved and no crystallization was observed.

Progressive dehydration of the latex sample leads to formation of an array of fairly ordered latex particles. After ~30 min of water evaporation, stage II is reached. Compared with the sample dispersed in water (Fig. 2), a significant amount of disordered array and salt residue is found in the electrolyte loaded system (Fig. 6). Furthermore, many latex particles are surrounded by very bright haloes which could not be removed by reduced water vapour pressure. Obviously, the water present in the interstitial space between the latex particles is so loaded with electrolytes that removal of the hydrophilic surface layer attached to the polymer particles is hindered.

In synthetic cement pore solution, the next stage of latex film formation which comprises particle coalescence towards a continuous polymer film is significantly retarded. After approximately 3 h only very minor particle deformation (stage II) was observed. The particles still exhibit their spherical shape while considerable efflorescence and crystallization of salts is evidenced (Fig. 7). Note that in the electrolyte-free aqueous systems, film formation has occurred already after ~60 min only (Fig. 3).

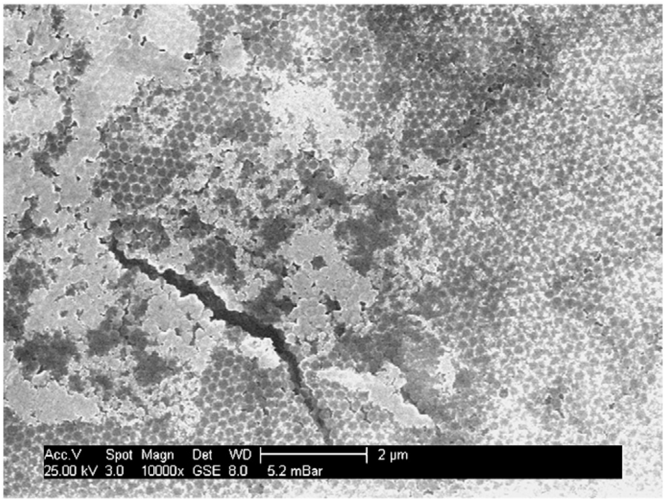

Fig. 6. ESEM micrograph of the latex sample after 30 min storage at 40 °C/25% r.h., dispersed in synthetic cement pore solution (stage II). Imaging conditions: $T = 3$ °C; $p = 5.2$ mbar; $U = 25$ kV; magnification: 10 000×.

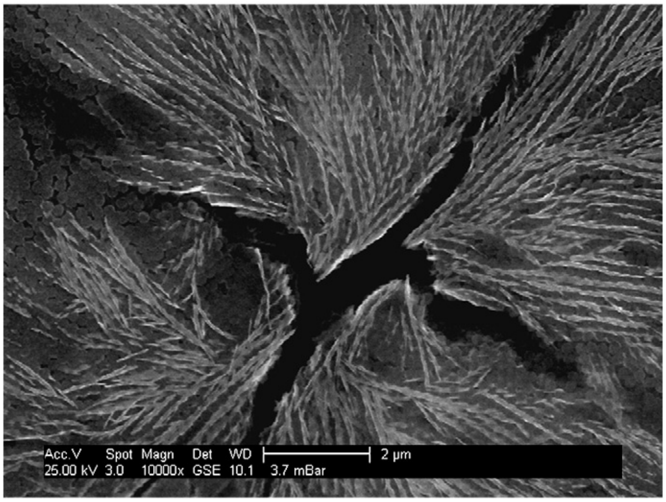

Fig. 7. ESEM micrograph of the latex sample after 3 h storage at 40 °C/25% r. h., dispersed in synthetic cement pore solution (stage II). Imaging conditions: $T = 3$ °C; $p = 3.7$ mbar; $U = 25$ kV; magnification: 10 000×.

After 24 h of drying, a gradual onset of latex deformation and polymer film formation was observed. Yet, still a large number of latex particles have maintained their individual shape and did not coalesce into a latex film. In order to determine the extent of film formation, the specimen was removed from the ESEM instrument and was rinsed once with ultrapure water to dissolve the salt layers. Even when low water vapour pressure ($p = 1.0$ mbar) was applied for imaging and thus enhanced evaporation rates for the water were to be expected, the particles still showed bright haloes (Fig. 8). This confirms that the layer of adsorbed water is particularly strong bound to the hydrophilic surfaces of the latex particles, and that only limited coalescence has occurred.

Apparently, the latex film forming process is severely retarded in cement pore solution, compared to the system with latex dispersed in water as solvent. In SCPS, completion of film formation was observed after ~3 days (Fig. 9). There, in contrast to the pure aqueous system, the polymer film is partially interspersed with large areas of bright residues resulting from hydrophilic membranes which contain adsorbed salts and emulsifier. These residues are interspersed with spherical cavities which can be attributed to the presence of latex spheres when salt precipitated during the drying and evaporation process. Elemental mapping by energy-dispersive X-ray diffraction (EDX) confirmed that inorganic salts were concentrated in the bright residues whereas practically no salts were found in the polymer latex film.

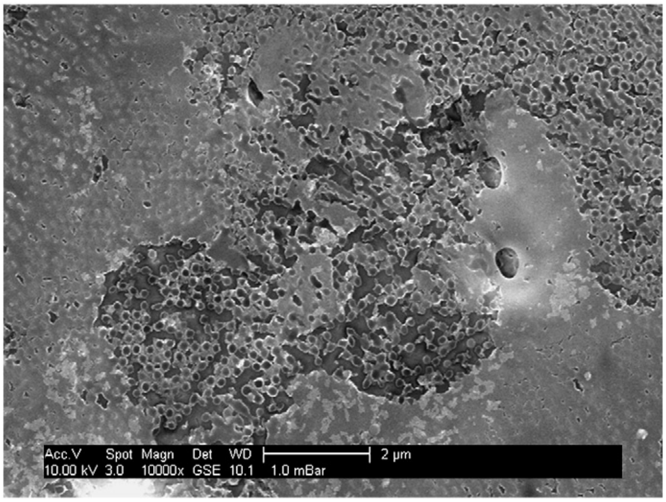

Fig. 8. ESEM micrograph of the latex sample dispersed in synthetic cement pore solution after 24 h of storage at 40 °C/25% r. h. after rinsing with water, exhibiting stages II, III and IV. Imaging conditions: $T = 3$ °C; $p = 1.0$ mbar; $U = 10$ kV; magnification: 10 000×.

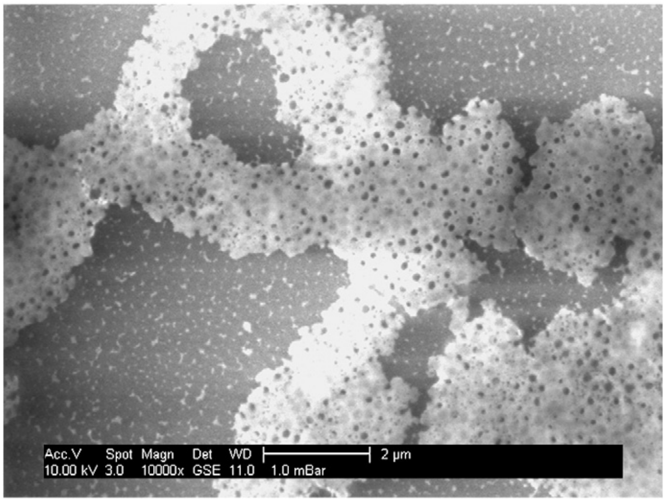

Fig. 9. ESEM micrograph of the latex sample dispersed in synthetic cement pore solution after 3 days of storage at 40 °C/25% r. h., showing a consistent polymer film (dark area) and large areas of separated salts and emulsifier (bright area, stage IV). Imaging conditions: $T = 3$ °C; $p = 1.0$ mbar; $U = 10$ kV; magnification: 10 000×.

The experiments allow to conclude that at 40 °C, film formation of the latex polymer is significantly retarded in the highly electrolyte loaded, alkaline pore solution. One explanation for this phenomenon is the precipitation of salts in the latex interstices during dehydration. This way, physical contact between the latex particles is hindered, resulting into a much reduced interdiffusion of polymer chains which is necessary to achieve film formation.

Additionally, the surface charge of the latex particles is influenced by pH and ion concentration present in the solvent. By using a particle charge detector (PCD) we have shown in previous work that the surface charge of those latex particles is strongly affected by pH [17]. At pH ≥ 6, deprotonation of the methacrylic acid starts and causes the surface charge of the latex to become increasingly negative. The maximum of the negative charge is reached at pH ~9.

The deprotonated carboxylate functionalities can strongly interact with cations present in the cement pore solution. There, especially complexation with Ca^{2+} ions is prevalent. Different types of Ca^{2+} coordination modes with carboxylate groups have been shown for polycarboxylate type superplasticizers to exist [18].

Here, interaction between cations present in the SCPS and the latex polymer was investigated by measurement of the streaming potential of the latex dispersion in presence of $CaCl_2$, NaCl and KCl. For this purpose, 0.25 mol/L aqueous salt solutions of $CaCl_2$, NaCl and KCl, respectively, were added stepwise to the latex dispersion containing 0.01 wt.% of polymer. The results are shown in Fig. 10. Apparently, the streaming potential is much influenced by the presence of those cations. Especially addition of Ca^{2+} ions reduces the surface charge of the latex particles exponentially from a highly negative value (~−1400 mV) towards the isoelectric point. This effect is owed to strong adsorption of Ca^{2+} ions onto the latex surface where oxygen donor atoms are present in the –COO^- functionalities and chelate the divalent cation. In comparison, interaction with monovalent cations such as Na^+ or K^+ is considerably less.

Obviously, surface adsorption of cations, particularly of Ca^{2+}, onto the latex polymer contributes much to the observed retardation of the film formation. Chelation of cations on the surfaces of the latex results into an expanded hydrophilic shell which is mainly occupied by a large number of Ca^{2+} ions. Those cations are in the way when polymer particles are to interdiffuse. Only when the pressure between particles becomes very high, then the layer of cations is giving way

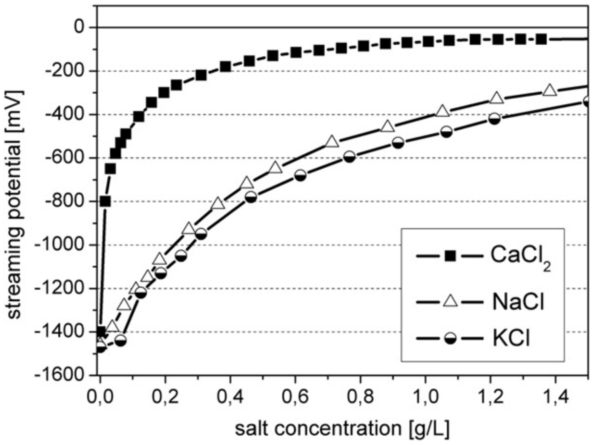

Fig. 10. Streaming potential of the synthesized anionic latex dispersion (concentration 0.01 wt.%) at different additions of salts and pH 12.6, determined in a particle charge detector.

and is excremented in the form of a salt deposit on the polymer film. This mechanism was observed by other authors who report that neutralization of the surface carboxylate groups of a methacrylic acid modified poly (butyl methacrylate) latex with divalent cations significantly reduces interdiffusion of the polymer chains, but does not entirely suppress latex film formation [19]. This effect explains the slower film formation observed in cement pore solution.

4. Conclusion

Our experiments indicate that in cementitious systems, film formation by latex polymers exhibiting carboxylate functionalities is severely retarded, compared to an almost electrolyte-free aqueous system.

By means of environmental scanning electron microscopy, time-dependent evolution of the latex polymer film occurring during storage at 40 °C/25% r. h. was monitored at certain time intervals. Using a specific pump-down sequence, the latex samples could be observed under the microscope without the risk of additional water loss stemming from the vacuum. For particles dispersed in water, the four characteristic stages of the film forming process were observed. Early in the dehydration process, a hydrophilic membrane is formed around the latex particles. It is enriched with anionic emulsifier and methacrylic acid. This hydrophilic membrane is clearly separated from the hydrophobic polymer core. Upon film formation, fragmentation of these membranes was observed. In aqueous solution, film formation already is completed after only ~4 h.

Using synthetic cement pore solution instead of water, the four different stages of latex coalescence into a polymer film were identified as well. The presence of high concentrations of electrolytes and strongly alkaline pH, however, severely retards the process of latex film formation. There, even after 24 h, particle coalescence is still in a premature state and requires ~3 days to be completed. One reason for this retardation is precipitation of salt from the solution during the dehydration process. This effect impedes direct contact between the latex spheres which is necessary for film formation. Another and potentially even stronger effect is owed to complexation of surface carboxylate groups by cations, particularly by Ca^{2+} ions. This chelating mechanism was evidenced by streaming potential measurement of the latex dispersion in presence of $CaCl_2$. There, almost complete charge neutralization occurs, due to the large amount of Ca^{2+} ions adsorbed. The layer of adsorbed cations retrieved from cement pore solution hinders polymer interdiffusion and subsequent polymer film formation.

These findings provide insight into the principle mechanism of latex film formation in cement-based building materials such as e.g. tile adhesives, self-levelling compounds and polymer concrete. There, when anionic latex dispersions are being used, a much retarded film formation and hence decreased cohesion and adhesion properties at the early stage can be expected. The extent of retardation mainly depends on the overall anionic surface charge of the latex dispersion, and the type of anionic groups present there. Functionalities possessing strong chelating properties for Ca^{2+} ions (e.g. phosphonate or acetyl acetonate groups) will retard more than weakly coordinating groups such as sulfonate and carboxylate. Whereas, the ion concentration present in cement pore solution which varies e.g. with the water-to-cement ratio exercises only a minor effect, because of continuous dissolution of Ca^{2+} ions which have been adsorbed by the latex dispersion.

Similar results as presented here for a synthetic model latex polymer were found for commercial anionic latex dispersions which are commonly used in mortars. There, the time difference required to achieve complete film formation in water and cement pore solution was comparable to that reported here. Our findings on the fundamentals of the latex coalescence process also apply to powder dispersions (so-called redispersible powders). Such powders contain polyvinylalcohol as a protective colloid to prevent film formation during spray-drying. This coating dissolves rapidly when the powder is added to aqueous cementitious systems. The subsequent coalescence process then follows the principle pattern described here.

Finally, it should be noted that our study presents the relative kinetics of latex coalescence under the conditions employed here (40 °C/25% r. h.) and for a latex of this specific chemical composition. Therefore, our study merely presents a qualitative, and not a quantitative idea about the kinetics of latex film formation in cement-based systems.

References

[1] J.B. Kardon, Polymer-modified concrete: review, J. Mater. Civ. Eng. 9 (1997) 85–92.
[2] Y. Ohama, Polymer-based admixtures, Cem. Concr. Comp. 20 (1998) 189–212.
[3] J.L. Keddie, Film formation of latex, Mat. Sci. Eng. Rep. 21 (1997) 101–170.
[4] P.A. Steward, J. Hearn, M.C. Wilkinson, An overview of polymer latex film formation and properties, Adv. Coll. Interf. Sci. 86 (2000) 195–267.
[5] Y. Chevalier, C. Pichot, C. Graillat, M. Joanicot, K. Wong, J. Maquet, P. Linder, B. Cabane, Film formation with latex particles, Colloid Polym. Sci. 270 (1992) 806–821.
[6] J.L. Keddie, P. Meredith, R.A. Jones, A.M. Donald, Kinetics of film formation in crylic latices studied with multiple-angle-of-incidence ellipsometry and environmental SEM, Macromolecules 28 (1995) 2673–2682.
[7] T.G. Fox, Influence of diluent and of copolymer composition on the glass temperature of a polymer system, Bull. Am. Phys. Soc. 1 (1956) 123–128.
[8] S. Chandra, P. Flodin, Interactions of polymers and organic admixtures on portland cement hydration, Cem. Concr. Res. 17 (1987) 875–890.
[9] S. Erkselius, L. Wadsö, O.J. Karlsson, Drying rate variations of latex dispersions due to salt induced skin formation, J. Coll. Interf. Sci. 317 (2008) 83–95.
[10] A. Jenni, L. Holzer, R. Zurbriggen, M. Herwegh, Changes in microstructures and physical properties of polymer-modified mortars during wet storage, Cem. Concr. Res. 36 (2006) 79–90.
[11] A.M. Donald, The use of environmental scanning electron microscopy for imaging wet and insulating materials, Nature Mat. 2 (2003) 511–516.
[12] D.J. Stokes, Recent advances in electron imaging, image interpretation and applications: environmental scanning electron microscopy, Phil. Trans. R. Soc. Lond. A 361 (2003) 2771–2787.
[13] R.E. Cameron, A.M. Donald, Minimizing sample evaporation in the environmental scanning electron microscope, J. Micros. 173 (1994) 227–237.
[14] W. Rechenberg, S. Sprung, Composition of the solution in the hydration of cement, Cem. Concr. Res. 13 (1983) 119–126.
[15] A.M. Donald, C. He, C.P. Royall, M. Sferrazza, N.A. Stelmashenko, B.L. Thiel, Applications of environmental scanning electron microscopy to colloidal aggregation and film formation, Colloids and Surfaces A, Physicochem. Eng. Asp. 174 (2000) 37–53.
[16] M. Joanicot, K. Wong, J. Richard, J. Maquet, B. Cabane, Ripening of cellular latex films, Macromolecules 26 (1993) 3168–3175.
[17] J. Plank, M. Gretz, Study on the interaction between anionic and cationic latex particles and Portland cement, Colloids and Surfaces A, Physicochem. Eng. Asp. 330 (2008) 227–233.
[18] J. Plank, B. Sachsenhauser, Experimental determination of the effective anionic charge density of polycarboxylate superplasticizers in cement pore solution, Cem. Concr. Res. 39 (2009) 1–5.
[19] H.B. Kim, M.A. Winnik, Effect of surface acid group neutralization on the interdiffusion rates in latex films, Macromolecules 27 (1994) 1007–1012.